The lipid composition of yeast cells modulates the response to iron deficiency

Tania Jordá[1], Antonia María Romero[1], Ana Perea-García[1], Nicolas Rozès[2] and Sergi Puig[1,#]

[1]Departamento de Biotecnología, Instituto de Agroquímica y Tecnología de Alimentos (IATA), Consejo Superior de Investigaciones Científicas (CSIC), Paterna, Valencia, Spain.

[2]Departament de Bioquímica i Biotecnología, Facultat d'Enologia, Universitat Rovira i Virgili, Tarragona, Spain.

To whom correspondence should be addressed:

Sergi Puig, Dept. Biotecnología, IATA-CSIC, Agustín Escardino 7, 46980, Paterna, Valencia, Spain. Tel: (+34) 963 900 022. Fax: (+34) 963 636 301. Email: spuig@iata.csic.es.

Abstract

Iron is a vital micronutrient for all eukaryotes because it participates as a redox cofactor in multiple metabolic pathways, including lipid biosynthesis. In response to iron deficiency, the *Saccharomyces cerevisiae* iron-responsive transcription factor Aft1 accumulates in the nucleus and activates a set of genes that promote iron acquisition at the cell surface. In this study, we report that yeast cells lacking the transcription factor Mga2, which promotes the expression of the iron-dependent Δ9-fatty acid desaturase Ole1, display a defect in the activation of the iron regulon during the adaptation to iron limitation. Supplementation with exogenous unsaturated fatty acids (UFA) or *OLE1* expression rescues the iron regulon activation defect of *mga2Δ* cells. These observations and fatty acid measurements suggest that the *mga2Δ* defect in iron regulon expression is due to low UFA levels. Subcellular localization studies reveal that low UFAs cause a mislocalization of Aft1 protein to the vacuole upon iron deprivation that prevents its nuclear accumulation. These results indicate that Mga2 and Ole1 are essential to maintain the UFA levels required for Aft1-dependent activation of the iron regulon in response to iron deficiency, and directly connect the biosynthesis of fatty acids to the response to iron depletion.

Highlights (3-5 sentences with max. 85 characters including spaces)

1) The yeast Mga2 transcription factor is required for the activation of the iron regulon.

2) The expression of *OLE1* rescues the *mga2Δ* defect on iron regulon activation.

3) Addition of linoleic acid rescues the *mga2Δ* defect on iron regulon activation.

4) Aft1 transcription factor mislocalizes to vacuoles in iron-deficient *mga2Δ* cells.

5) The *AFT1-1*^{up} allele rescues *mga2Δ* phenotypes on iron-deficient conditions.

Keywords: yeast, *Saccharomyces cerevisiae*, iron deficiency, fatty acids, Aft1, Mga2, Ole1.

Abbreviations: BPS, bathophenanthroline disulfonic acid disodium; ChIP, chromatin immunoprecipitation; DIC, differential interference contrast; ER, endoplasmic reticulum; FAS, ferrous ammonium sulfate; FeRE, Iron regulatory element; GFP, green fluorescent protein; Pol II, polymerase II; OD, optical density; RT-qPCR, Real Time - quantitative Polymerase Chain Reaction; SC, synthetic complete; SFA; saturated fatty acid; TM, transmembrane; UFA, unsaturated fatty acid.

1. Introduction

Biological membranes are selective and dynamic barriers composed of proteins and lipids, which cooperate to define the physicochemical properties that contribute to organelle identity and function. Environmental and metabolic stresses trigger alterations in the lipid composition of membranes with the purpose of adapting cellular homeostasis [1]. The budding yeast *Saccharomyces cerevisiae* is a powerful model organism to study multiple aspects of membrane biology [2]. In yeast, unsaturated fatty acid (UFA) [palmitoleic (16:1) and oleic (18:1)] biosynthesis from the corresponding saturated fatty acid (SFA) [palmitic (16:0) and stearic (18:1)] is catalyzed by the essential Δ9-fatty acid desaturase Ole1 [3]. Ole1 is a conserved iron- and oxygen-dependent enzyme whose expression is regulated by two homologous and partially redundant transcription factors, Mga2 and Spt23 (reviewed in [4-6]). Both Mga2 and Spt23 are synthesized as inactive dimer precursors anchored to the endoplasmatic reticulum (ER) membrane and, in response to different stimuli, are released by a proteolytic cleavage, resulting in a truncated polypeptide that translocates to the nucleus and activates *OLE1* transcription via low oxygen regulatory elements (LOREs) and fatty acid regulated (FAR) regions [7-13]. The activation of both transcription factors requires specific ubiquitylation by the E3 ligase Rsp5, processing by the proteasome, and mobilization from the ER membrane by the segregase/chaperone complex $Cdc48^{Npl4/Ufd1}$ [7-12]. Although each transcription factor is sufficient for *OLE1* expression, Mga2 is the dominant factor that activates *OLE1* expression in response to changes in temperature, oxygen or UFA levels [7, 13-16]. Recent data have demonstrated that Mga2 does not act as a sensor of membrane

fluidity; instead a bulky tryptophan residue situated deep in its transmembrane helix senses the surrounding molecular lipid-packing density of the ER membrane [17]. Thus, a more saturated ER membrane increases the packing of the membrane and causes the sensory tryptophan to rotate away from the lipid bilayer and towards the dimer interface, leading to the proteolytic activation of Mga2 [6, 17, 18]. We have recently shown that a decrease in the bioavailability of iron leads to changes in the UFA/SFA balance that activate *OLE1* transcription in an Mga2-dependent manner [19]. Consistent with this, *mga2Δ* cells display an important growth defect under iron-deficient conditions unless UFAs are added to the medium or *OLE1* is ectopically expressed [19].

Iron is an essential micronutrient that participates as a vital cofactor in multiple metabolic pathways, including lipid biosynthesis. Accordingly, iron deficiency leads to a decrease in yeast UFA, sterol and sphingolipid biosynthetic pathways [19, 20]. Iron deficiency is the most frequent nutritional disorder worldwide due to the extremely low solubility of iron under aerobic and physiological conditions. *S. cerevisiae* cells utilize two partially redundant transcription factors, Aft1 and Aft2, to regulate the response to iron deficiency (reviewed in [21]). Aft1 and Aft2 do not respond directly to environmental or intracellular iron levels, but rather to the efficiency of Fe-S cluster synthesis in mitochondria [22]. Under iron replete conditions, Aft1 and Aft2 proteins sense a mitochondrial iron signal that keeps them shuttling between the nucleus and the cytoplasm [22-25]. When iron bioavailability decreases, Aft1 and Aft2 transcription factors accumulate in the nucleus and bind to conserved iron-responsive element (FeRE) sites within the promoter of target genes to activate transcription [24, 26, 27]. Aft1 and Aft2 target approximately 35 genes,

collectively known as the iron regulon, which include: the high-affinity iron uptake system at the plasma membrane, composed of Fet3 and Ftr1; the family of cell surface iron siderophore transporters Arn1-4; and the cell wall mannoproteins Fit1-3, which facilitate iron uptake (reviewed in [28, 29]). *AFT1* alleles insensitive to iron, such as *AFT1-1*^{up}, constitutively express the iron regulon regardless of iron concentration [26].

In this study, we investigated why cells lacking the Mga2 transcription factor do not properly activate the iron regulon upon iron scarcity. Evidence indicates that the altered FA composition of *mga2Δ* cells leads to Aft1 mislocalization to the vacuole when iron is scarce, contributing to the *mga2Δ* growth defect under iron deficiency.

2. Materials and Methods

2.1. Yeast strains, culture conditions and plasmids

The *S. cerevisiae* strains and plasmids used in this study are listed in Supplemental Table S1. Yeast precultures were cultivated overnight at 30°C in liquid synthetic complete (SC) medium [0.17% yeast nitrogen base without amino acids and without ammonium sulfate (Pronadisa), 0.5% ammonium sulfate (Panreac), 2% glucose (Panreac), and 2 g/L Kaiser drop-out (Formedium)] lacking specific requirements when necessary, and reinoculated at an OD_{600} of 0.2. Then, yeast cells were incubated for 6 h at 190 rpm in SC medium (+Fe) or SC supplemented with 100 µM of the Fe^{2+}-specific chelator bathophenanthroline disulfonic acid disodium (BPS) (Sigma) to create iron deficiency (-Fe). The temperature sensitive mutant strains *pre1-1*, *rsp5-2* and *npl4-1* were cultivated as previously described [19]. To induce P_{GAL1}-*OLE1* expression, glucose in SC was replaced by 2% galactose. Linoleic acid (18:2, Sigma) was added to 1 mM final concentration and was stabilized with 1% Tergitol Nonidet P-40 (Sigma). The Fe^{2+}-specific chelator Ferrozine (Sigma) was used at the indicated concentration to limit iron bioavailability in 2% agar (Pronadisa) solid SC media. For growth assays in solid media, yeast cells were cultivated to exponential phase, spotted in 10-fold serial dilutions starting at on OD_{600} of 0.1, incubated at 30°C for 3 days, and photographed.

2.2. RNA analyses

Total RNA isolation and cellular mRNA levels were determined by RT-qPCR as previously described [30]. Primers used for RT-qPCR are listed in Supplemental Table S2.

2.3. Protein analyses

Total protein extractions were performed with the alkali method as previously described [31]. Proteins were resolved in SDS-PAGE gels and transferred to nitrocellulose membranes. Aft1-tagged proteins were detected with anti-HA (3F10, Sigma) and anti-GFP (Roche) primary antibodies. Pgk1 protein, used as a loading control, was detected with anti-Pgk1 (22C5D8; Invitrogen) antibody. Images were obtained with an ImageQuant LAS 4000 mini Biomolecular Imager (GE Healthcare Life Sciences).

Chromatin immunoprecipitation (ChIP) assays to determine RNA polymerase II binding to *FET3* and *FUS1* promoters were performed as previously described [32]. Cell extracts were incubated with Dynabeads Pan Mouse IgG (Invitrogen) previously bound to a monoclonal mouse anti-Rpb1 antibody (clone 8WG16, Covance). DNA was purified with the High Pure PCR Product Purification Kit (Roche). Primers used for gene promoter RT-qPCR analyses are listed in Supplemental Table S2.

2.4. Determination of total fatty acids

The fatty acid methyl ester analysis was performed as previously reported [19].

2.5. β-galactosidase assays

β-galactosidase activity was measured as previously described [33].

2.6. Fluorescence Microscopy

Differential interference contrast and GFP fluorescence images were captured on an Eclipse 90i Nikon microscope (Nikon corporation, Japan) using a digital camera (Nikon DS-5Mc). For cell quantification, more than 100 cells from at least 3 independent experiments were scored as cells with a predominantly cytoplasmic, nuclear or vacuolar signal. Vacuoles (one or more per cell) may appear as clear indentations in differential interference contrast (DIC) images. To stain the vacuolar membrane, exponentially growing cells were concentrated 20-fold and FM4-64 was added to a final concentration of 8 μM. Cells were incubated for 15 min in agitation at 30ºC, washed once with SC-ura, and incubated in SC-ura for an additional hour.

2.7. Statistical analyses

To evaluate statistical significance, tailed t-student tests were applied. Different letters above the bars represent significant differences among group. When the statistical test indicates that two means are significantly different from each other (P value < 0.05), they are labeled with different letters over the bars. When there are no significant differences, at least one letter over the two bars is the same.

3. Results

3.1. Genetic iron-dependent interaction between aft1Δ and mga2Δ mutants.

Previous studies support a link between lipid metabolism and the response of yeast cells to iron deficiency [19, 20, 34, 35]. For instance, the synthesis of unsaturated fatty acids (UFAs) decreases when iron is scarce [19, 20]. We have recently demonstrated that the decrease in the unsaturated/saturated fatty acid (UFAs/SFAs) ratio that occurs upon iron depletion promotes the cleavage of the Mga2 transcription factor from the ER membrane [19]. The released Mga2 travels to the nucleus and activates *OLE1* transcription to compensate the changes in the lipid composition of membranes [19]. Thus, cells deleted for *MGA2* gene display a strong growth defect under iron deficiency probably due to the lack of *OLE1* expression [19, 36]. Genome-wide approaches indicate that there is a genetic interaction between *mga2Δ* cells and mutants in the main iron-responsive transcription factor Aft1 [37, 38]. To specifically test this phenotype, we constructed an *mga2Δaft1Δ* double mutant and assayed for growth on synthetic complete SC medium. No growth differences were observed between wild-type, *aft1Δ and mga2Δ* strains on SC, whereas the *mga2Δaft1Δ* double mutant exhibited an important growth defect (Fig. 1). Importantly, the growth defect displayed by the *mga2Δaft1Δ* mutant was fully rescued by the addition of iron to the growth medium (Fig. 1). This and previous observations [19] strongly suggest that Mga2 contributes to the response of yeast cells to changes in iron bioavailability.

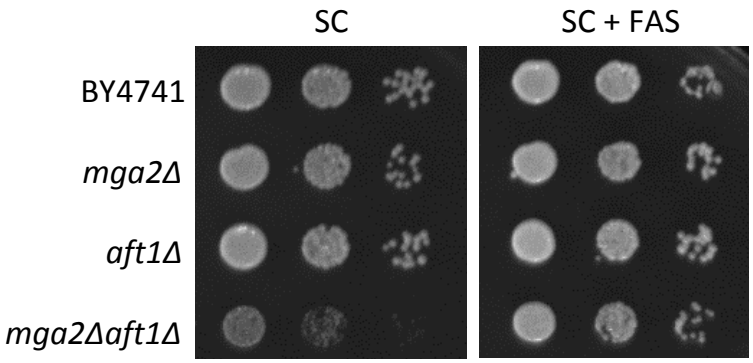

Fig. 1. Iron rescues the negative genetic interaction between *aft1Δ* and *mga2Δ* mutants. Wild-type (BY4741), *mga2Δ* (SPY824), *aft1Δ* (SPY28), and *mga2Δaft1Δ* (SPY992) cells were assayed for growth in SC and SC supplemented with 300 μM ferrous ammonium sulfate (+FAS). Plates were incubated at 30ºC for 3 days and photographed. A representative experiment of four biologically independent assays is shown.

3.2. The Mga2 transcription factor is required for the correct activation of the iron regulon in response to iron deficiency.

To investigate the molecular role played by Mga2, and its paralog Spt23, in the response of yeast cells to iron deficiency, we cultivated wild-type (BY4741), *mga2Δ* and *spt23Δ* cells under iron-sufficient (+Fe) or iron-deficient (−Fe) conditions and determined the mRNA levels of several members of the iron regulon by RT-qPCR. As expected, *FET3*, *FTR1*, *FIT3, ARN2 and FIT1* mRNA levels increased upon iron deprivation conditions in wild-type cells (Fig. 2). Interestingly, the up-regulation of these iron regulon genes upon iron depletion was importantly affected in *mga2Δ* cells, whereas only a slight defect was observed in the *spt23Δ* mutant (Fig. 2). We were unable to investigate the expression of the iron regulon in cells lacking both transcription factors because the *mga2Δspt23Δ* double mutant is unviable [7, 39]. These results suggest that

Mga2 and, to a minor extent, Spt23 transcription factors are required for the correct activation of the iron regulon in response to iron deficiency.

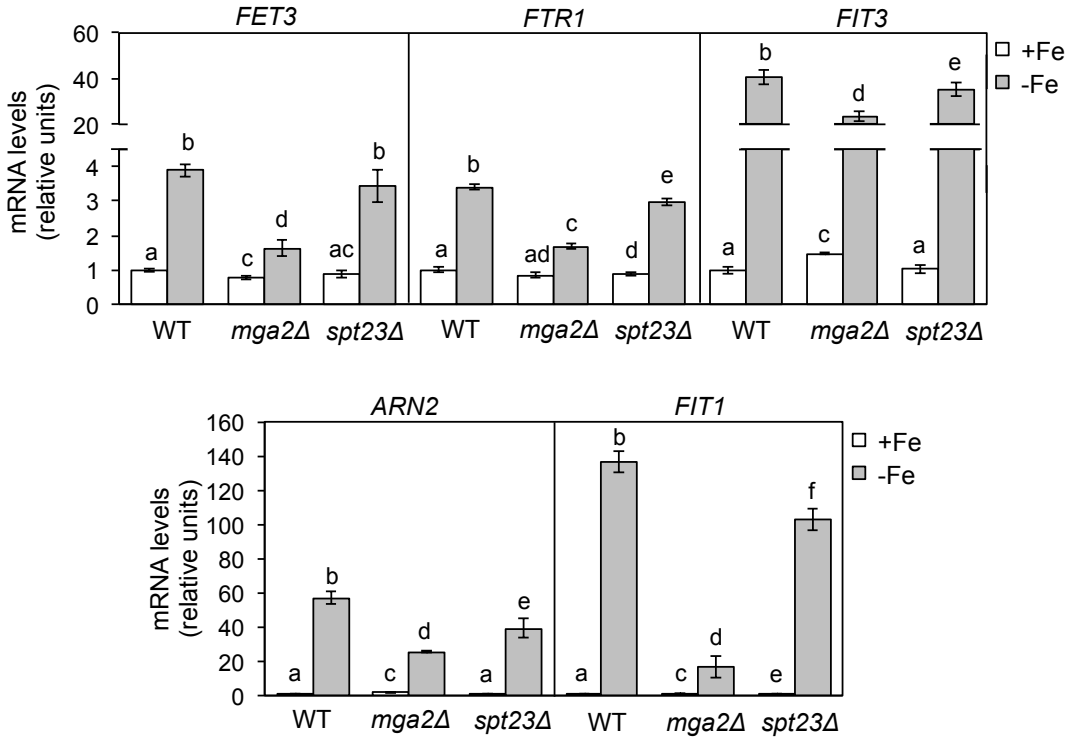

Fig. 2. The activation of the iron regulon by iron deficiency is defective in *mga2Δ* mutant cells. Wild-type (WT), *mga2Δ* (SPY824), and *spt23Δ* (SPY823) cells were cultivated at 30 °C for 6 hours to exponential phase in SC medium without (+Fe) or with 100 µM BPS (-Fe). Total RNA was extracted, and *FET3*, *FTR1*, *FIT3*, *ARN2* and *FIT1* mRNA levels normalized to *PGK1* mRNA were determined by RT-qPCR as described in Materials and Methods. Data show the average and standard deviation of three biologically independent experiments relative to the wild-type strain grown in +Fe conditions. Different letters above the bars represent statistically significant differences (p-value < 0.05).

To further assess the implication of Mga2 in the mechanism of activation of the iron regulon when iron is scarce, we investigated the contribution of its cleavage from the ER membrane. The release of Mga2 from the ER membrane requires the proteasome, the E3 ubiquitin ligase Rsp5 and the segregase complex $Cdc48^{Npl4/Ufd1}$ [8, 9, 12]. Given that *PRE1*, *RSP5* and *NPL4* genes are essential in yeast, we used cells expressing the temperature-sensitive alleles *pre1-1, rsp5-2* and *npl4-1*, which are defective in the proteasome, Rsp5 and the segregase, respectively. For these and further studies we focused on three members of the iron regulon: *FET3*, *FTR1* and *FIT3*. Whereas *FET3*, *FTR1* and *FIT3* transcript abundance importantly increased in response to iron deficiency in all the wild-type strains cultivated at the non-permissive temperature of 37ºC, a significantly smaller iron regulon induction was observed for the *pre1-1, rsp5-2* and *npl4-1* mutants (Fig. 3A-C). Thereby, the proteasome, Rsp5 and $Cdc48^{Npl4/Ufd1}$ are required for iron regulon activation by iron depletion probably due to its contribution to the release of Mga2 from the ER membrane.

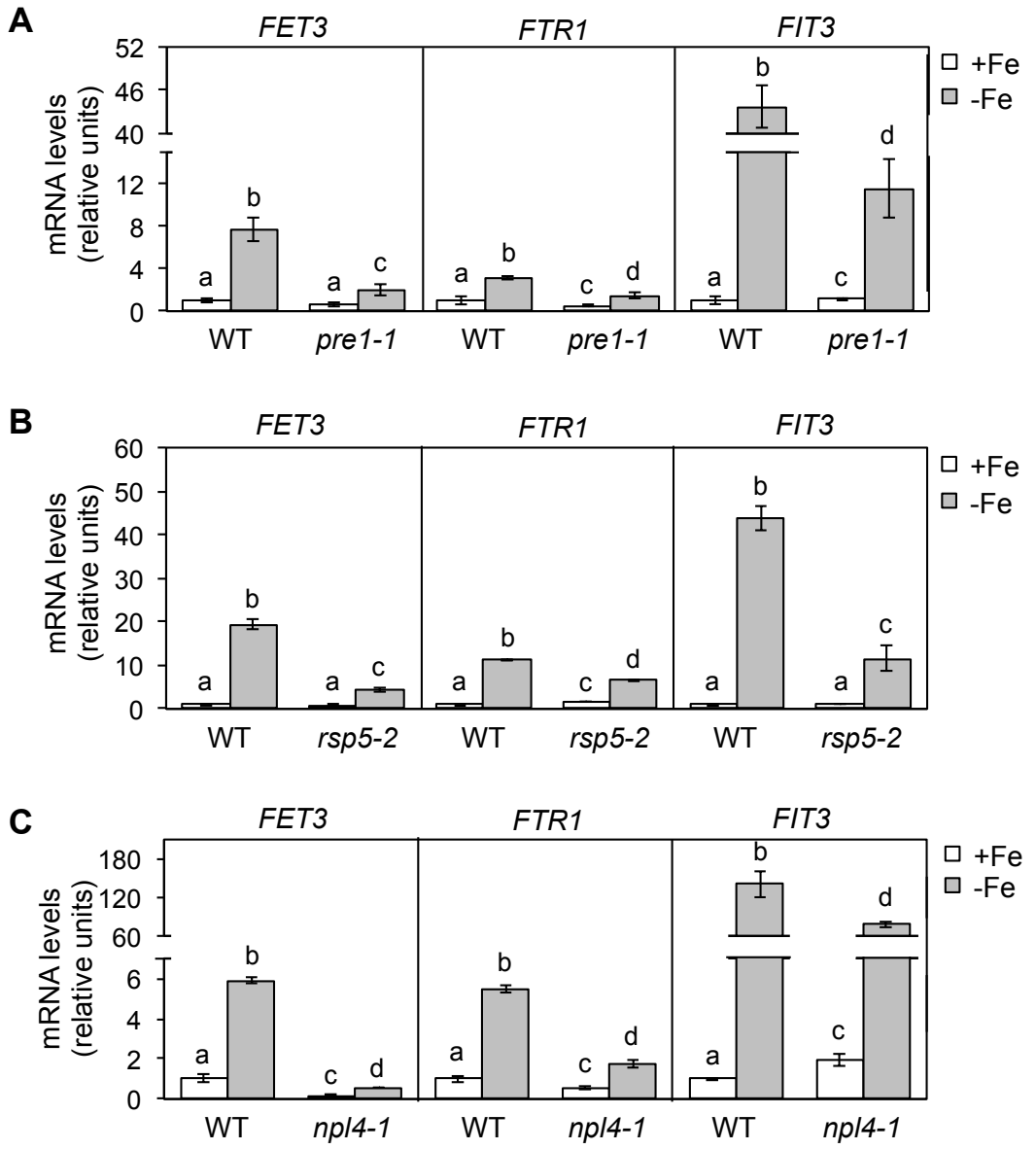

Fig. 3. The proteasome, the E3 ubiquitin ligase Rsp5 and Npl4 are required for the correct activation of the iron regulon upon iron depletion. (A) The proteasome is required for the activation of the iron regulon by low iron. Wild-type (WT, YWO0607) and *pre1-1* (YWO0608) cells were cultivated overnight at 25 °C in SC and then transferred to 37 °C for 1 h. Then, 100 µM BPS was added (−Fe) or not (+Fe), and cells were incubated for 5 additional hours. (B) The E3 ubiquitin ligase Rsp5 facilitates the induction of the iron regulon in response to iron depletion. Wild-type (WT, Y0356) and *rsp5-2* (Y0358) cells were cultivated as described in panel A. (C) The substrate-

recruiting cofactor of the $Cdc48^{Npl4/Udf1}$ is required to activate the expression of the iron regulon upon iron limitation. Wild-type (WT, PSY580) and *npl4-1* (PSY2340) cells were cultivated overnight at 25 °C in SC and then transferred to a medium without (+Fe) or with 100 µM BPS (-Fe) at 30 °C for 6 hours. In all cases, total RNA was extracted and *FET3*, *FTR1* and *FIT3* mRNA levels, normalized to *PGK1* mRNA, were determined by RT-qPCR. Data indicate the average and standard deviation of three biologically independent experiments referred to the corresponding wild-type strain cultivated in +Fe conditions. Different letters above the bars represent statistically significant differences (p-value < 0.05).

Next, we determined the transcript levels of these iron regulon genes in *mga2Δ* cells that expressed a wild-type Mga2 protein (*MGA2*) or an Mga2 protein without its ER-anchoring transmembrane (TM) domain (*MGA2ΔTM*). We observed similar levels of the iron regulon transcripts in both strains under +Fe and –Fe conditions (Fig. 4A). Therefore, the soluble Mga2ΔTM protein counteracts the iron regulon activation defect observed in *mga2Δ* cells upon iron scarcity, but does not activate by itself the iron regulon in iron replete conditions (Fig. 4A). These results indicate that the release of Mga2 from the ER is necessary, but not sufficient, to induce the iron regulon. Finally, we assayed growth in iron-deficient conditions and observed that the expression of *MGA2ΔTM* was able to rescue the growth defect of *mga2Δ* cells (Fig. 4B).

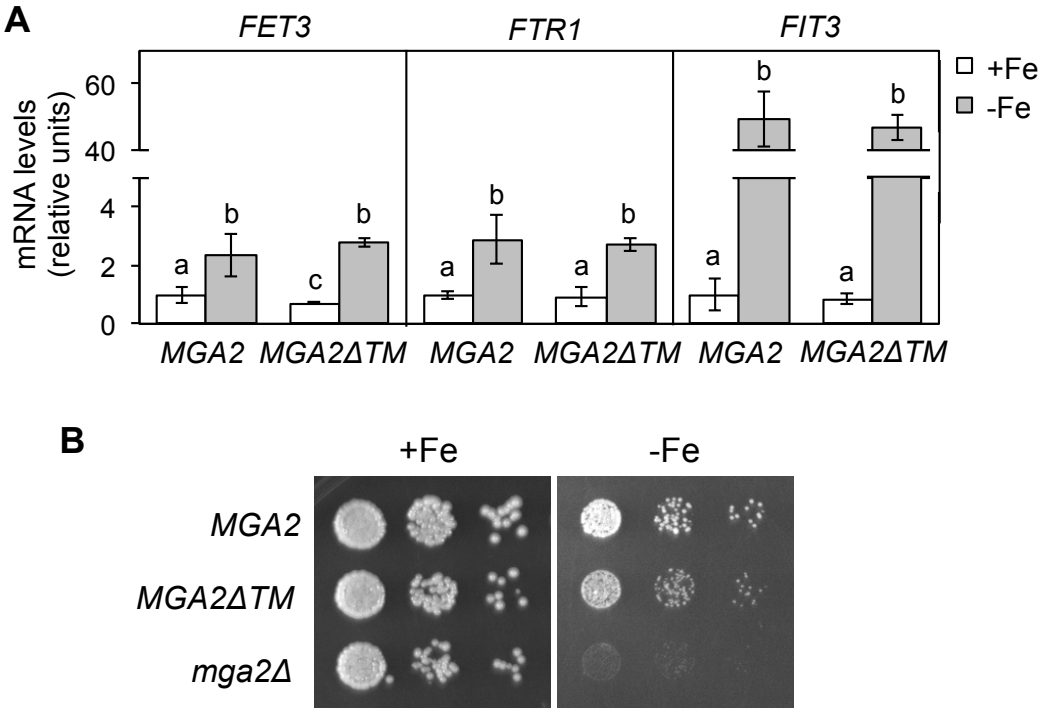

Fig. 4. An Mga2 protein lacking its transmembrane domain rescues the phenotypes of *mga2Δ* cells under low iron conditions (A) *MGA2ΔTM* rescues the activation of the iron regulon. Yeast *mga2Δ* (SPY824) cells transformed with pPS2364 (*MGA2*) or pPS2358 (*MGA2ΔTM*) plasmids were cultivated, processed and analyzed as described in Fig. 2. Data indicate the average and standard deviation of three biologically independent experiments, relative to wild-type strain grown in +Fe conditions. Different letters above the bars represent statistically significant differences (*p*-value < 0.05). (B) *MGA2ΔTM* rescues the growth defect of *mga2Δ* cells in low iron. Yeast *mga2Δ* (SPY824) cells transformed with pPS2364 (*MGA2*), pPS2358 (*MGA2ΔTM*) or pRS416 (*mga2Δ*) plasmids were assayed for growth in SC (+Fe) and SC supplemented with 400 μM of ferrozine (-Fe). Plates were incubated at 30ºC for 3 days and photographed. A representative experiment of four biologically independent assays is shown.

3.3. OLE1 expression rescues the defect of iron regulon activation displayed by mga2Δ cells.

We have earlier demonstrated that Mga2 is essential for growth in media with low iron bioavailability because of defects in *OLE1* expression and UFA synthesis [19]. Therefore, we hypothesized that the lack of *OLE1* expression and the decrease in UFA synthesis could be the reason underneath the defect in iron regulon induction displayed by *mga2Δ* cells. To test it, we expressed *OLE1* under the control of the galactose-inducible and glucose-repressed *GAL1* promoter (P_{GAL1}-*OLE1* construct) in wild-type and *mga2Δ* cells. Cells were cultivated in an iron-sufficient (+Fe) or iron-deficient galactose medium without glucose. We first verified by RT-qPCR that both WT and *mga2Δ* cells containing the P_{GAL1}-*OLE1* construct expressed higher *OLE1* mRNA levels than cells containing empty vector (Fig. 5A). Then, we examined the *FET3*, *FTR1* and *FIT3* transcript levels (Fig. 5B-5D). As previously shown for glucose-containing media (Figs. 2 and 3), the iron regulon mRNA levels increased upon iron depletion in wild-type cells when cultivated in galactose media, but were defective in the *mga2Δ* mutants. Moreover, the artificial expression of *OLE1* did not alter the induction of the iron regulon upon iron limitation in WT cells (Fig. 5). Importantly, the expression of *OLE1* with the *GAL1* promoter rescued the iron regulon activation defect observed in *mga2Δ* cells (Fig. 5). These results indicate that the defect of activation of the iron regulon displayed by the *mga2Δ* mutant is due to a lack of *OLE1* expression.

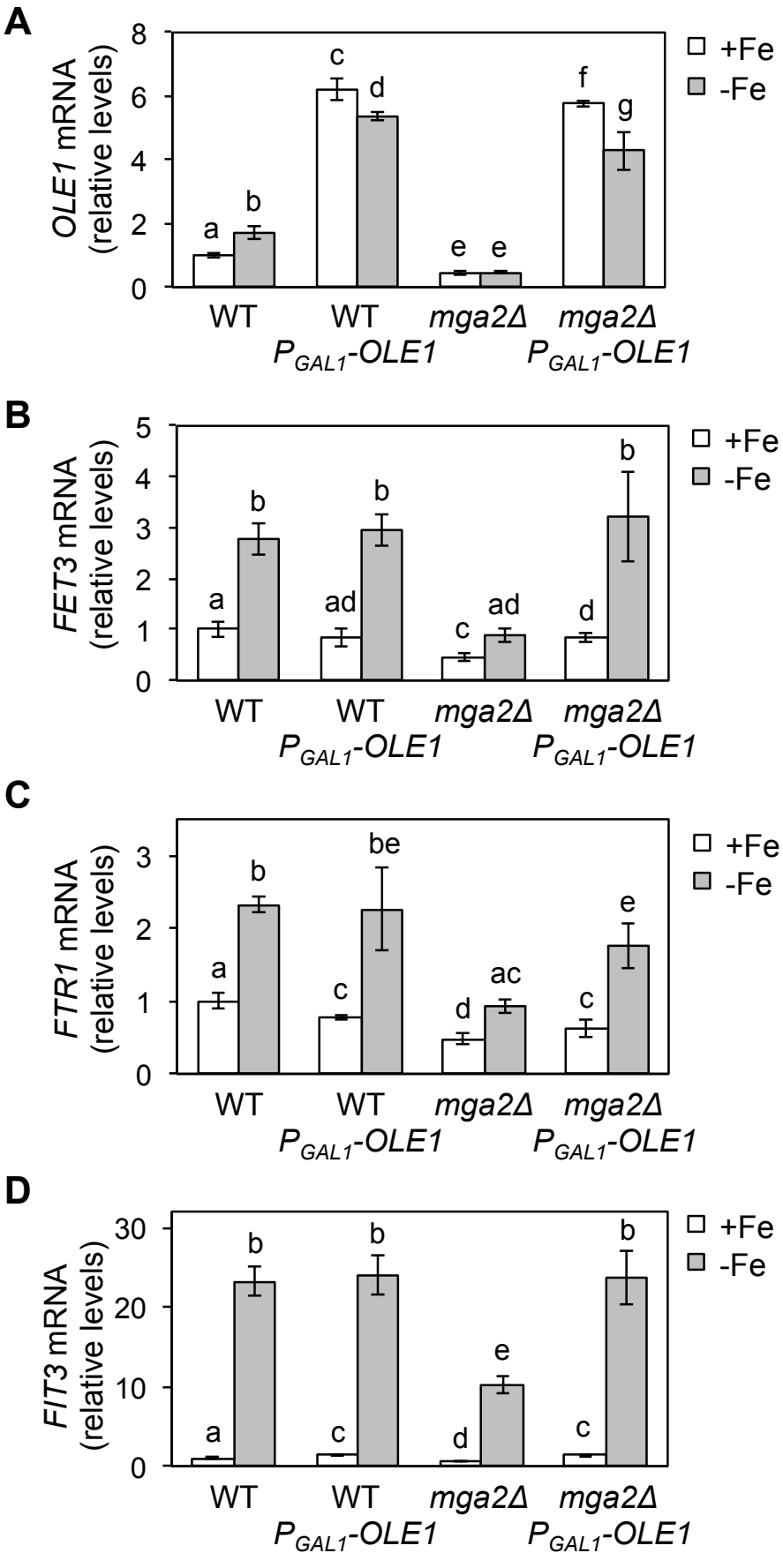
A
OLE1 mRNA (relative levels)
8
6
4
2
0
a
b
c
d
e
e
f
g
+Fe
-Fe
WT
WT
mga2Δ
mga2Δ
P_GAL1-OLE1
P_GAL1-OLE1
B
FET3 mRNA (relative levels)
5
4
3
2
1
0
a
b
ad
b
c
ad
d
b
+Fe
-Fe
WT
WT
mga2Δ
mga2Δ
P_GAL1-OLE1
P_GAL1-OLE1
C
FTR1 mRNA (relative levels)
3
2
1
0
a
b
c
be
d
ac
c
e
+Fe
-Fe
WT
WT
mga2Δ
mga2Δ
P_GAL1-OLE1
P_GAL1-OLE1
D
FIT3 mRNA (relative levels)
30
20
10
0
a
b
c
b
d
e
c
b
+Fe
-Fe
WT
WT
mga2Δ
mga2Δ
P_GAL1-OLE1
P_GAL1-OLE1

Fig. 5. The *GAL1*-driven expression of *OLE1* rescues the defect in iron regulon activation of *mga2Δ* cells Wild-type (WT, BY4741) and *mga2Δ* (SPY824) cells transformed with either pRS416 empty vector or pRS316-P_{GAL1}-OLE1 plasmid were cultivated overnight at 30 ºC in SC-ura with 2% raffinose instead of glucose and then transferred to SC-ura with 2% galactose in absence (+Fe) or presence of 100 µM BPS (-Fe) for 6 hours to induce *OLE1* expression. Total RNA was extracted, and *OLE1* (A), *FET3* (B), *FTR1* (C) and *FIT3* (D) mRNA levels normalized with *PGK1* mRNA were determined by RT-qPCR. Data indicate the average and standard deviation of three biologically independent experiments, relative to wild-type cells cultivated in +Fe conditions. Different letters above the bars represent statistically significant differences (*p*-value < 0.05).

3.4. The defect of mga2Δ cells in iron regulon activation is due to low UFA levels.

Since Ole1 desaturase is necessary for UFA synthesis, we decided to determine the total fatty acid (FA) composition of wild-type and *mga2Δ* mutant cells under both +Fe and –Fe conditions. As previously reported for glucose media [19], we observed that the total UFA abundance in relation to SFA levels diminished in a wild-type strain when cultivated in a galactose iron-limited medium (Fig. 6A). The decrease in UFA/SFA abundance was more dramatic in *mga2Δ* cells mostly due to the drop in abundance of palmitoleic acid levels (16:1) and an augment of stearic (18:0) and palmitic acid (16:0) (Fig. 6A and Supplemental Fig. S1). The over-expression of *OLE1* with the *GAL1* promoter increased the UFA/SFA ratio of both wild-type and *mga2Δ* cells cultivated under iron-sufficient conditions (Fig. 6A). More important, *OLE1* overexpression under iron replete conditions enabled the recovery of the UFA/SFA abundance of an

mga2Δ mutant to levels similar to those of the wild-type strain (Fig. 6A and Supplemental Fig. S1).

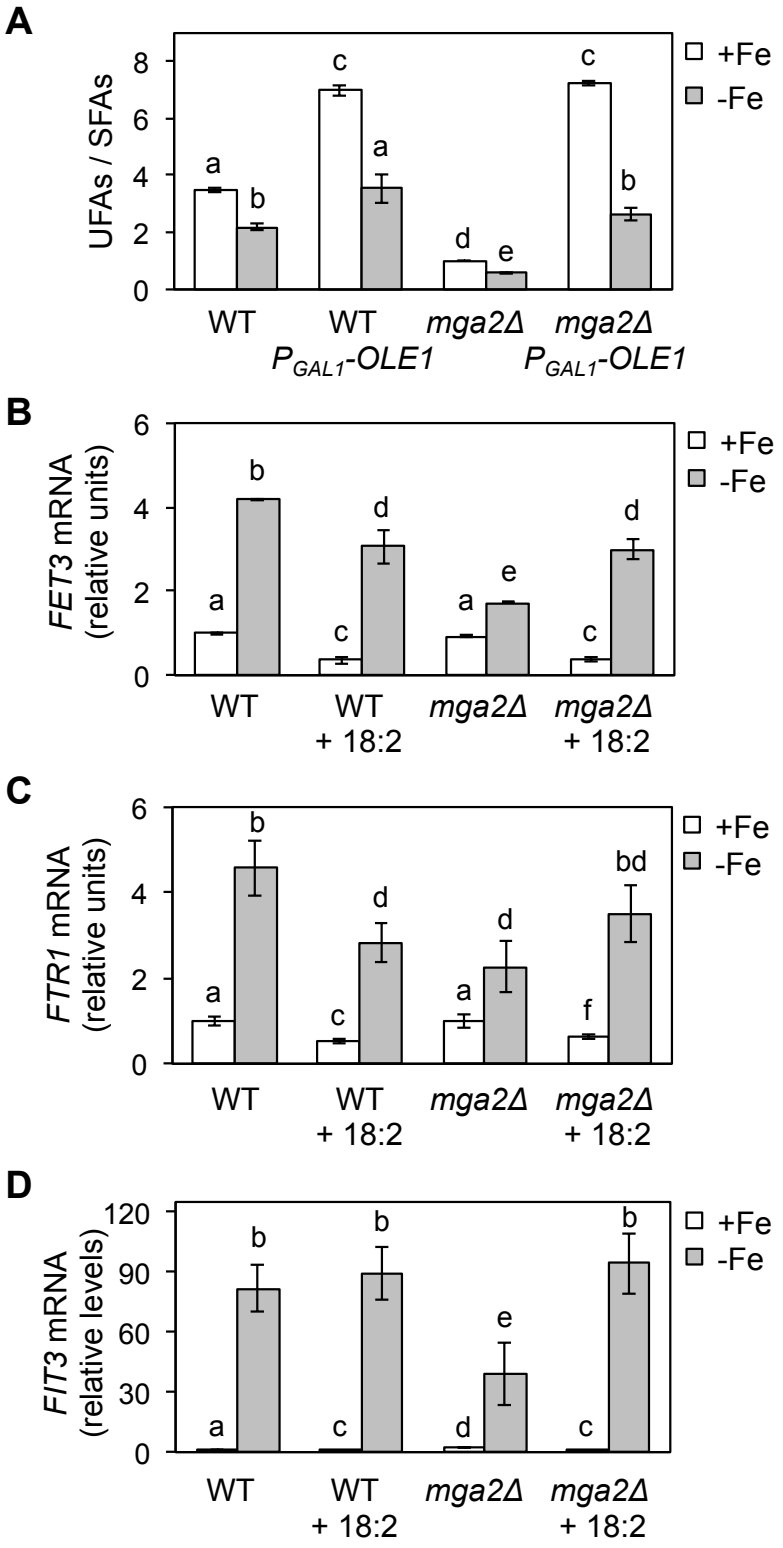

Fig. 6. UFA supplementation reverts the iron regulon activation defect of *mga2Δ* cells. (A) The *GAL1*-driven expression of *OLE1* increases the UFA/SFA ratio of *mga2Δ* cells. Wild-type (WT, BY4741) cells transformed with pRS416 or pRS316-P_{GAL1}-OLE1 plasmids were cultivated as described in Fig. 5. The percentage of UFAs and SFAs was determined as described in Materials and Methods, and the UFAs/SFAs ratio was represented. (B-D) Wild-type (WT, BY4741) and *mga2Δ (*SPY824) cells were cultivated at 30 °C for 6 hours in SC (+Fe) or SC + 100 µM BPS (−Fe) without or with 1 mM linoleic acid (+18:2). Total RNA was extracted and *FET3* (B), *FTR1* (C) and *FIT3* (D) mRNA levels normalized with *PGK1* mRNA were determined by RT-qPCR. Transcript values are shown as relative to the WT (+Fe) samples. In all cases, data indicate the average and standard deviation of three biologically independent experiments. Different letters above the bars represent significant differences (*p*-value < 0.05).

To further ascertain whether the defect in activation of the iron regulon observed in the *mga2Δ* mutant was due to low UFA levels, we supplemented the growth medium with linoleic acid (18:2), an UFA that cannot be synthesized by *S. cerevisiae* but is incorporated into the membrane lipids, and determined the iron regulon mRNA levels by RT-qPCR in wild-type and *mga2Δ* cells under both +Fe and –Fe conditions (Fig. 6B-6D and Supplemental Fig. S1). The expression levels of *FET3* and *FTR1* slightly decreased in wild-type cells under both iron sufficient and replete conditions (Fig. 6B and 6C), whereas no effect was observed on *FIT3* expression (Fig. 6D). We also analyzed other members of the iron regulon and observed that the addition of linoleic acid to wild-type cells slightly decreased *ARN2* and increased *FIT1* mRNA levels under iron deficiency (Supplemental Fig. S1). Importantly, the defect of activation of the iron regulon upon iron deficiency displayed by the *mga2Δ* mutant was partially or fully rescued by linoleic acid supplementation (Fig. 6B-6D and Supplemental

Fig. S1). Collectively, these results indicate that the iron regulon expression defect of *mga2Δ* cells is probably a consequence of defects in UFA synthesis due to low *OLE1* expression.

3.5. Mga2 facilitates the activation of FET3 upon iron deficiency by enhancing the recruitment of the RNA pol II to its promoter.

In response to iron deficiency, the Aft1 transcription factor associates to the promoter of iron regulon genes to activate transcription [25, 27]. To address whether the defect of iron regulon activation displayed by *mga2Δ* cells depended on the promoter region, we transformed wild-type and *mga2Δ* cells with a plasmid containing the sequence of *FET3* promoter, which is mostly regulated by Aft1 [40], fused to the *lacZ* reporter gene (P_{FET3}-*lacZ*) and performed β-galactosidase activity assays under both +Fe and –Fe conditions. As previously reported [26], the expression of P_{FET3}-*lacZ* was induced in wild-type cells under iron-limited conditions (Fig. 7A). However, P_{FET3}-*lacZ* induction by iron deficiency diminished in *mga2Δ* cells (Fig. 7A). To further study the contribution of *FET3* promoter to the Mga2 effect, we determined the recruitment of RNA Pol II to *FET3* promoter by chromatin immunoprecipitation (ChIP) in both wild-type and *mga2Δ* cells cultivated in +Fe and −Fe conditions (Fig. 7B). Consistently with an increase in transcription, iron starvation stimulated the occupancy of the *FET3* promoters by RNA Pol II (Fig. 7B). Conversely, an important defect on the recruitment of the RNA Pol II to the *FET3* promoter was observed in *mga2Δ* cells when iron was scarce (Fig. 7B), which suggests a failure in the transcriptional activation of *FET3* gene in *mga2Δ*

cells. Altogether, these results suggest that Mga2 modulates the expression of the iron regulon genes via their promoter region.

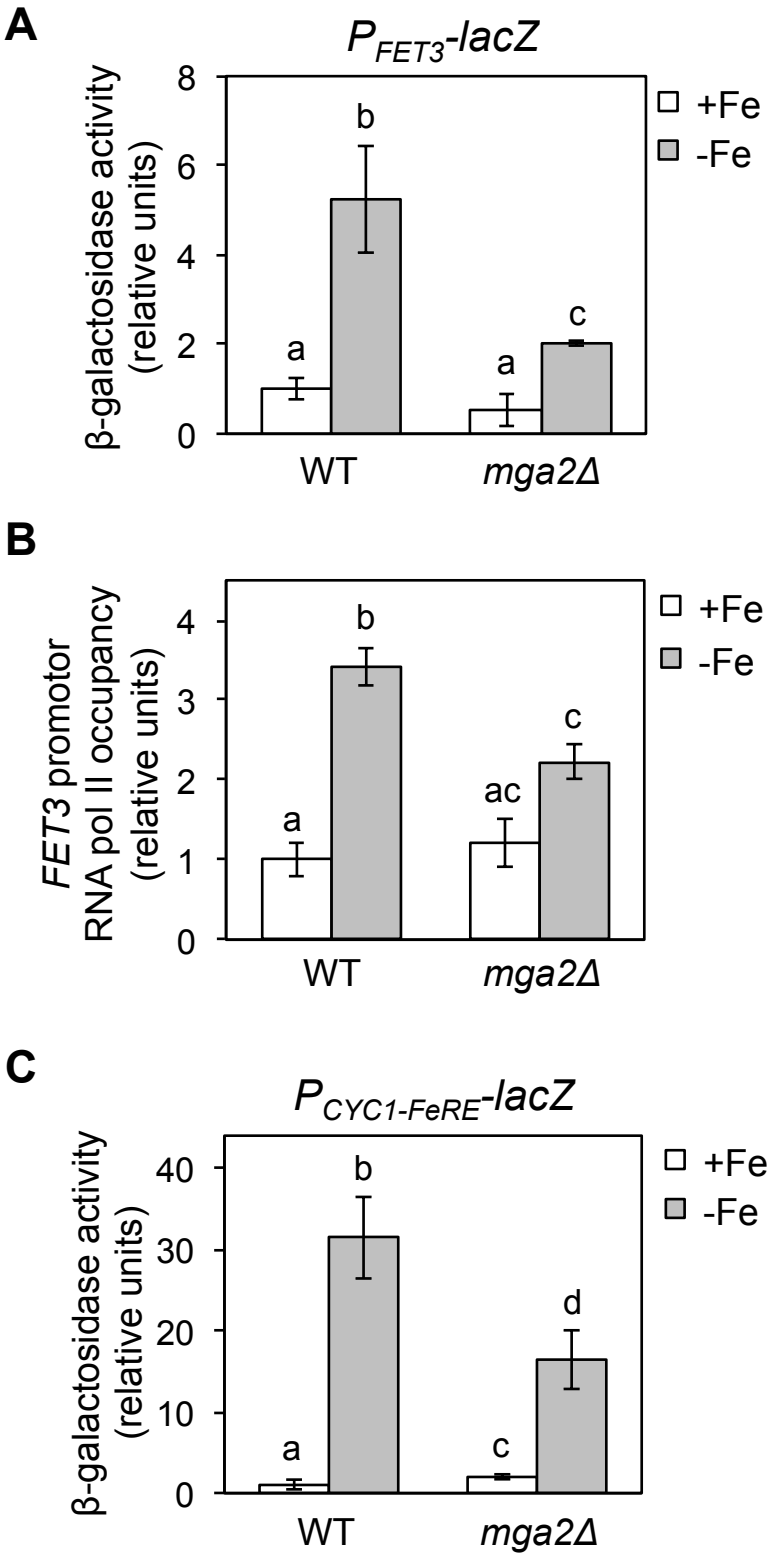

Fig. 7. Mga2 activates *FET3* expression upon iron depletion via FeREs. (A) Mga2-mediated activation of *FET3* expression by low iron occurs through its promoter. Wild-type (WT, BY4741) and *mga2Δ* (SPY824) cells transformed with P174 (P_{FET3}-*lacZ*) plasmid were cultivated as described in Fig. 1 and β-galactosidase activity was determined. (B) Mga2 facilitates the recruitment of RNA Pol II to the *FET3* promoter upon low iron. Wild-type (WT, BY4741) and *mga2Δ* (SPY824) cells were cultivated as described in Fig. 1. Proteins were extracted and immunoprecipitated with anti-RNA Pol II monoclonal antibody, and binding to *FET3* promoter region normalized to *FUS1* promoter was determined by RT-qPCR. (C) The Mga2-dependent activation of transcription depends on FeRE sites. Wild-type (WT, BY4741) and *mga2Δ* (SPY824) cells transformed with pSP441 ($P_{CYC1\text{-}FeRE}$--lacZ) plasmid were cultivated and analyzed as described in panel A. All data represent the average and standard deviation of three biologically independent experiments, in relation to the WT (+Fe) samples. Different letters above the bars represent significant differences (*p*-value < 0.05).

The promoters of the iron regulon genes contain FeRE sites that are required for Aft1 binding and activation of transcription [27]. To investigate whether Mga2 facilitates the activation of transcription via FeREs, we used a plasmid expressing *lacZ* under the control of the *CYC1* promoter fused to two FeRE sequences ($P_{CYC1\text{-}FeRE}$-*lacZ*). Wild-type and *mga2Δ* cells expressing $P_{CYC1\text{-}FeRE}$-*lacZ* were cultivated in +Fe and –Fe conditions and β-galactosidase activity was determined. As previously reported [41], the fusion of FeRE sites to the *CYC1* promoter conferred iron deficiency up-regulation to the *CYC1* promoter (Fig. 7C). Importantly, the activation of *lacZ* via FeRE was defective in the *mga2Δ* mutant (Fig. 7C). These results suggest that Mga2 facilitates the activation of the iron regulon upon iron depletion via FeREs.

3.6. Aft1 mRNA and protein levels do not diminish in mga2Δ cells.

A potential explanation for the iron-regulon activation defect that *mga2Δ* cells display in response to iron depletion could be a decrease in *AFT1* expression when Mga2 is not present. To ascertain how Mga2 influences *AFT1* abundance, we cultivated both wild-type and *mga2Δ* mutant cells in +Fe and –Fe conditions in the absence or presence of linoleic acid (18:2), and we determined *AFT1* mRNA and protein levels by RT-qPCR and Western blot, respectively (Fig. 8). Interestingly, we observed a slight increase in both *AFT1* mRNA and protein levels in response to iron deficiency, which was not affected by linoleic acid. Basal *AFT1* mRNA levels were similar between wild-type and *mga2Δ* mutants, and only a slight up-regulation was observed for iron-depleted *mga2Δ* cells (Fig. 8A). Importantly, *mga2Δ* cells displayed lightly higher Aft1 protein levels than wild-type cells in all conditions (Fig. 8B). Although the molecular reasons for these small changes are not known, we can conclude that Aft1 protein levels do not decrease in *mga2Δ* cells, and consequently do not provide by themselves support for a defect in the activation of the iron regulon upon iron scarcity.

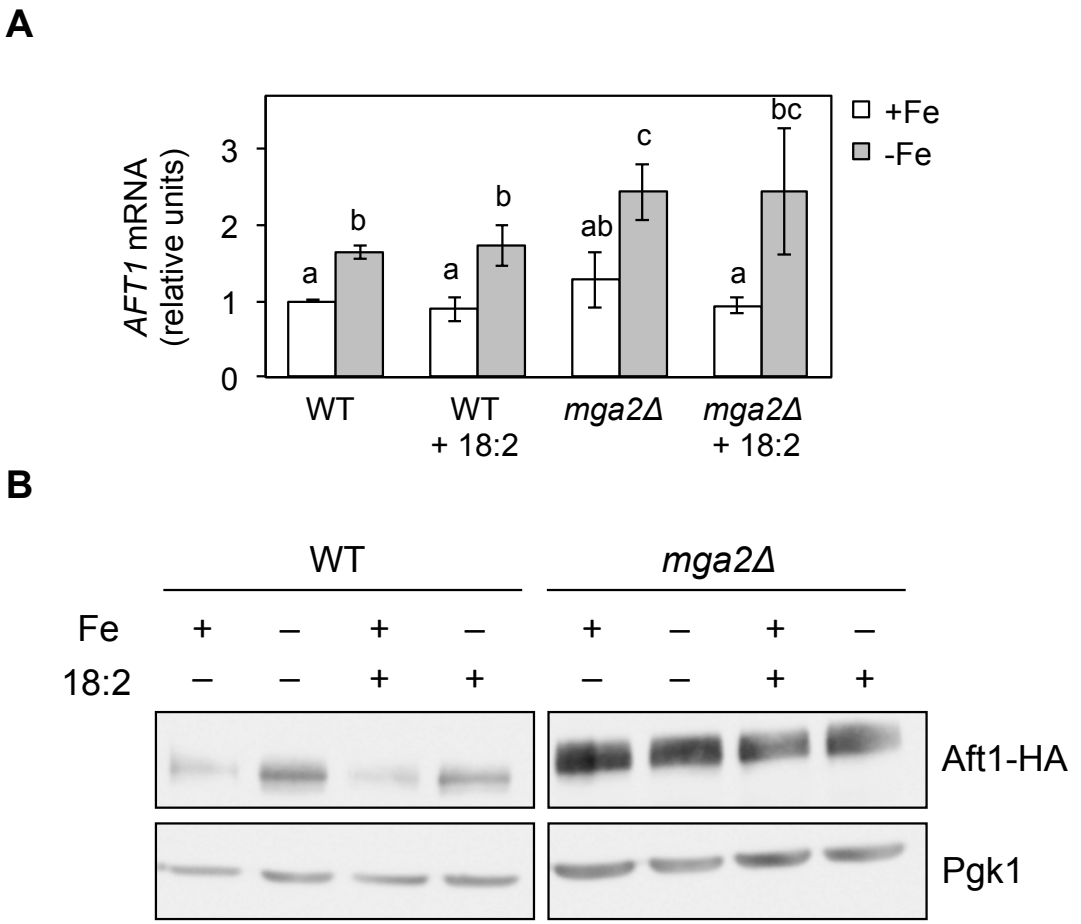

Fig. 8. *AFT1* expression levels in *mga2Δ* cells. (A) *AFT1* mRNA levels. Wild-type (WT, BY4741) and *mga2Δ (*SPY824) cells were cultivated as described in Fig. 6B. Total RNA was extracted and *AFT1* mRNA levels normalized with *PGK1* mRNA were determined by RT-qPCR. Transcript values are shown as relative to the WT (+Fe) samples. In all cases, data indicate the average and standard deviation of three biologically independent experiments. Different letters above the bars represent significant differences (*p*-value < 0.05). (B) Aft1 protein levels. *aft1Δ* (SPY28) and a*ft1Δmga2Δ (*SPY992) mutant cells transformed with pRS416-AFT1-12HA plasmid were cultivated as described in Fig. 6B. Aft1-HA and Pgk1 protein levels were analyzed by Western blot with anti-HA and anti-Pgk1 antibodies, respectively. A representative experiment of two biological replicates is shown.

3.7. Aft1 localization is altered in mga2Δ cells under iron deficiency.

Under iron replete conditions, Aft1 protein shuttles between the nucleus and the cytoplasm. However, when iron bioavailability is restricted, Aft1 accumulates in the nucleus, activating the expression of the iron regulon [24, 27]. In order to investigate the cause of the decrease in Aft1 activity in *mga2Δ* cells, we used a high-copy plasmid previously characterized that expresses a functional GFP-Aft1 fusion protein [42]. First, we determined GFP-Aft1 protein abundance in wild-type and *mga2Δ* cells cultivated in +Fe and −Fe conditions. We observed an up-regulation of Aft1 protein levels in response to iron depletion in both strains (Supplemental Fig. S2). Then, we analyzed the subcellular localization of GFP-Aft1 protein in both wild-type and *mga2Δ* cells cultivated in +Fe and −Fe conditions by fluorescence microscopy. As expected, GFP-Aft1 increased its nuclear localization when wild-type cells were cultivated in iron-deficient conditions (Fig. 9A; WT cells). Importantly, GFP-Aft1 protein was predominantly mislocalized in *mga2Δ* cells cultivated under iron-depleted conditions, leading to a decreased nuclear localization (Fig. 9A; *mga2Δ* cells). Colocalization of GFP-Aft1 protein with the lipophilic dye FM4-64, which selectively localizes to the vacuolar membrane under our assay conditions (see Materials and Methods), indicated that *mga2Δ* cells accumulate Aft1 protein in the vacuole when iron bioavailability is limited (Fig. 9B). Quantification of these observations confirmed that *mga2Δ* cells were defective in the accumulation of Aft1 into the nucleus when iron was scarce, leading to its mislocalization to the vacuole. Moreover, consistent with a rescue of the iron-regulon up-regulation defect of *mga2Δ* cells (Fig. 6), the supplementation with linoleic acid increased the accumulation of Aft1 in the nucleus of *mga2Δ* cells upon iron starvation (Fig.

9A and 9C; *mga2Δ* –Fe + 18:2 cells). These results strongly suggest that the defect in expression of the iron regulon displayed by *mga2Δ* cells is due to an alteration in Aft1 subcellular localization, which is probably a consequence of a decrease in the UFAs present in cellular membranes.

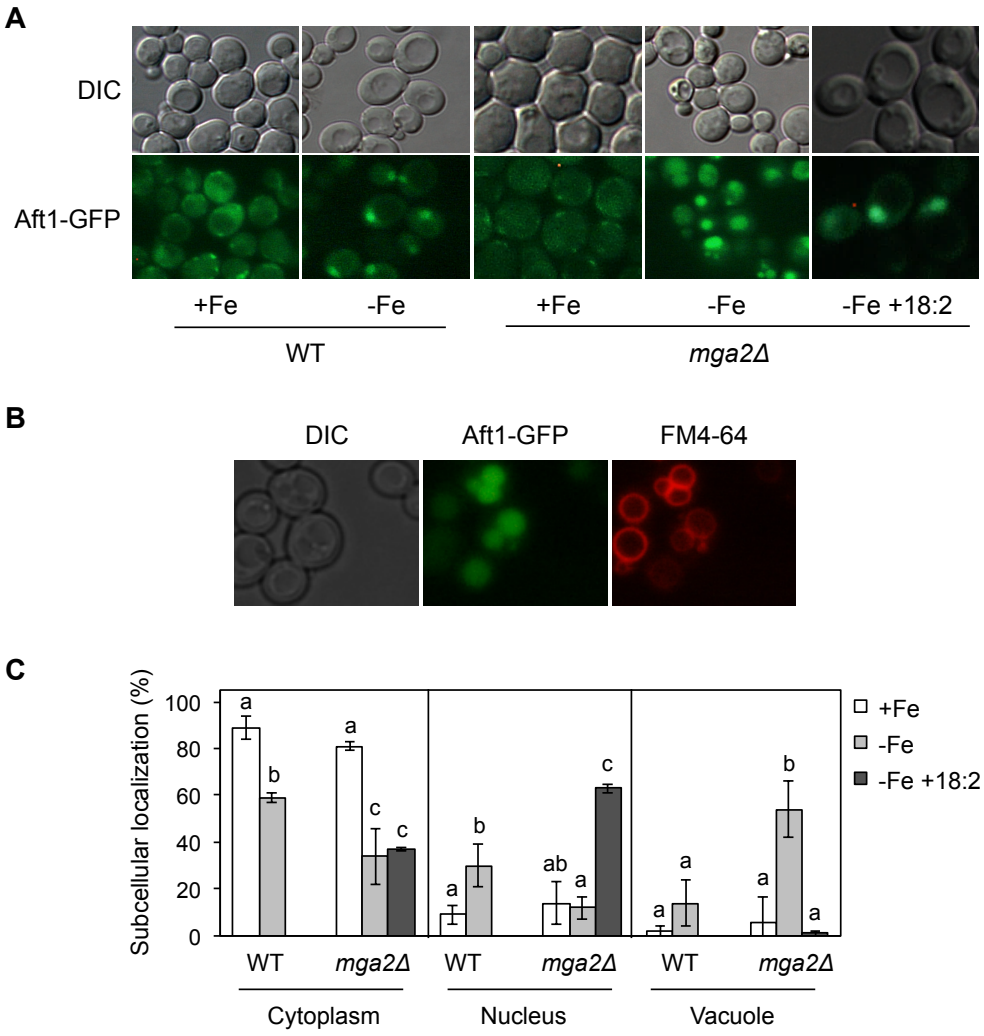

Fig. 9. Aft1 localization is altered in *mga2Δ* cells upon iron limitation. (A) Wild-type (WT, BY4741) and *mga2Δ* (SPY824) cells containing JK1346 (pRS426-GFP-AFT1) plasmid were cultivated for 6 hours to exponential phase in SC-ura with 20 µM FAS (+Fe) or 100 µM BPS (−Fe). Then, cells were visualized under Nomarski (DIC) and GFP fluorescence optics. (B) The vacuolar membrane of *mga2Δ* (SPY824) cells expressing GFP-Aft1 and cultivated in iron-deficient conditions were stained with the styryl dye FM4-64 as indicated in Materials and Methods. (C) Quantitative analysis of Aft1 subcellular

localization patterns in the WT and *mga2Δ* cells. More than 100 cells were counted for three biologically independent experiments. Aft1 subcellular distribution patterns were classified as predominantly cytoplasmic, nuclear or vacuolar. The average and standard deviation were represented. Different letters above the bars represent significant differences (p-value < 0.05).

3.8. A constitutively nuclear Aft1 protein rescues the phenotypes of mga2Δ cells under iron deficiency.

As an attempt to rescue the Aft1 nuclear accumulation defect of the *mga2Δ* mutant, we used an Aft1 protein (Aft1-1^{up}) that is constitutively nuclear and activates the iron regulon expression regardless of the cellular iron status [26]. For this purpose, wild-type and *mga2Δ* cells transformed with either empty vector or an *AFT1-1^{up}*-containing plasmid were cultivated under +Fe and –Fe conditions and the mRNA level of members of the iron regulon determined. As shown in the Fig. 1 (SC medium), the transcript levels of the iron regulon genes analyzed increased under iron depletion in wild-type cells when iron was scarce, and this activation was defective in *mga2Δ* mutants (Fig. 10A, SC-ura medium). As expected, when *AFT1-1^{up}* was expressed in *mga2Δ* cells under iron-sufficient conditions, *FET3*, *FTR1* and *FIT3* transcript levels raised compared to the wild-type cells cultivated under the same conditions (Fig. 10A). Importantly, the expression of the *AFT1-1^{up}* allele rescued the iron regulon up-regulation defect displayed by *mga2Δ* cells under iron starvation (Fig. 10A).

Previous data reported that *mga2Δ* cells exhibit an important growth defect under iron-deficient conditions [19, 36]. This growth defect is fully rescued by expressing *OLE1* under the control of the *GAL1* promoter [19]. To

explore a potential contribution of Aft1 mislocalization to *mga2Δ* growth defect under low iron conditions, we tested whether *AFT1-1^{up}* could rescue *mga2Δ* growth phenotype. Importantly, we observed that *AFT1-1^{up}* partially or fully recovered the growth defect displayed by the *mga2Δ* mutant cultivated in solid and liquid iron-deficient media (Fig. 10B and 10C). These results indicate that the growth defect displayed by *mga2Δ* mutants under low iron conditions is, at least partially, due to a defect in Aft1 accumulation in the nucleus caused by diminished levels of UFAs.

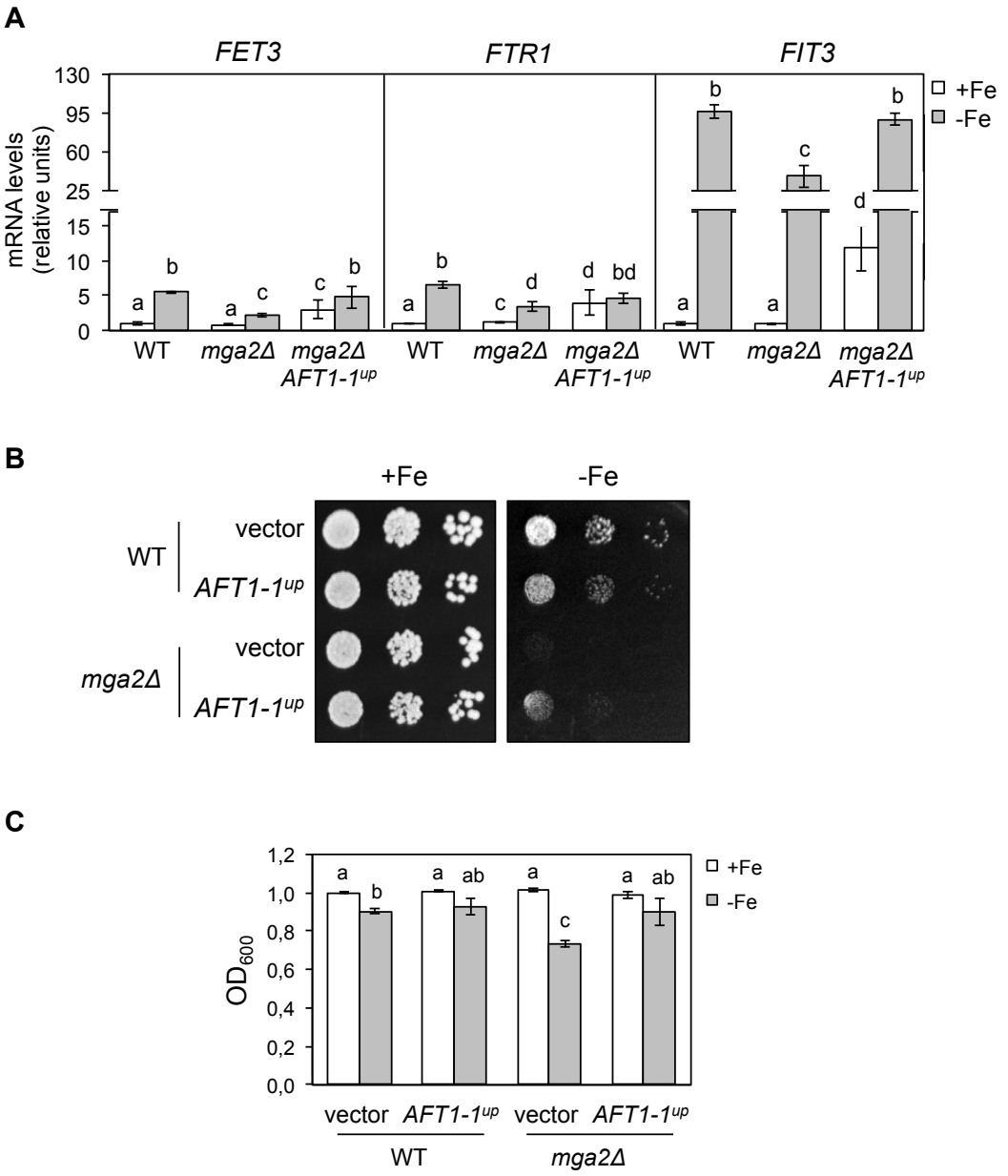

Fig. 10. The *AFT1-1^{up}* allele rescues the phenotypes of *mga2Δ* under iron depletion. Wild-type (WT, BY4741) and *mga2Δ* (SPY824) cells were transformed with either pRS416 (vestor) or pRS416-AFT1-1^{up}-12HA (AFT1-1^{up}) plasmids. (A) The *AFT1-1^{up}* allele rescues the activation of the iron regulon upon iron depletion. Cells were cultivated in SC-ura as described in Fig. 1. Total RNA was extracted, and the *FET3*, *FTR1* and *FIT3* mRNA levels normalized with *PGK1* mRNA were determined by RT-qPCR. (B) *AFT1-1^{up}* allele partially rescues the growth defect of *mga2Δ* cells on iron-depleted solid medium. Cells were cultivated overnight and spotted on SC-ura (+Fe) and SC-ura with 600 µM Ferrozine (-Fe). Plates were incubated at 30ºC and photographed. (C) *AFT1-1^{up}* allele rescues the growth defect of *mga2Δ* cells on iron-depleted liquid medium. Cells were cultivated at 28ºC in 96-well plates containing SC-ura and SC-ura with 150 µM BPS as described in Materials and Methods. The OD_{600} after 60 hours is represented. In panels A and C, data indicate the average and standard deviation of three biologically independent experiments, and different letters above the bars represent significant differences (*p*-value < 0.05).

4. Discussion

The biosynthesis of UFAs depends on a conserved Δ9-fatty acid desaturase, known as Ole1 in yeast and SCD1 in mammals, that coordinates an oxo-diiron prosthetic group essential for catalysis [4, 5]. We have recently described that, when iron bioavailability decreases, yeast Δ9-fatty acid desaturase activity diminishes leading to low UFA synthesis [19]. This causes the release of the Mga2 transcription factor from the ER membrane and the consequent activation of *OLE1* expression [19]. We showed that the defect in UFA synthesis that *mga2Δ* mutants exhibited in iron-deficient conditions limited growth, which could be rescued by UFA supplementation or *OLE1* expression [19]. However, it was unknown how a decrease in UFAs specifically affected

mga2Δ cells under iron deficiency. Here, we have shown that *mga2Δ* cells and mutants defective in Mga2 release from the ER membrane limit the activation of the iron regulon (Figs. 2 and 3). Previous studies have demonstrated that the expression of an Mga2 protein lacking its ER-anchoring domain (Mga2ΔTM) activates *OLE1* expression [7, 19]. However, we have observed that this is not the case for the iron regulon, since Mga2ΔTM-expressing cells do not activate the iron regulon under iron-sufficient conditions more than wild-type cells (Fig. 4A). These results suggested that Mga2 was necessary but not sufficient for the activation of the iron regulon. Similarly to its growth defect ([19]; Fig. 4B), the restricted expression of iron regulon genes displayed by *mga2Δ* cells was complemented by UFA addition, *OLE1* or *MGAΔTM* expression (Figs. 4-6). Altogether, these observations suggested that Mga2 was not directly activating the iron regulon, but rather indirectly altering the FA composition of yeast cells, which ultimately would reduce the response to iron deficiency.

Aft1 and Aft2 are the transcription factors that modulate the response of yeast cells to iron depletion by binding to FeRE sites within the promoter region of target genes and activating transcription [27, 40, 43]. Aft1 plays the dominant role, whereas Aft2 mostly regulates the expression of intracellular iron transporters [44, 45]. By using an Aft1-target gene, *FET3*, we have shown that Mga2 facilitates the activation of the iron regulon via FeRE sequences by recruiting the RNA pol II to their promoters, which strongly indicates that Mga2 exerts its effect through Aft1 transcription factor (Fig. 7). We considered the possibility that Mga2 activates the expression of *AFT1* in response to iron deficiency. However, no defects in Aft1 mRNA and protein levels were observed in *mga2Δ* mutants (Fig. 8); instead a slight increase in Aft1 abundance was

obtained probably due to Aft1 vacuolar accumulation or other indirect effects. Aft1 is a nucleocytoplasmic protein that accumulates in the nucleus when iron bioavailability decreases ([24]; Fig. 9). No significant differences in the subcellular localization of Aft1 protein were observed between wild-type and *mga2Δ* cells under iron replete conditions, suggesting that Aft1 shuttling was not affected by the lack of Mga2 (Fig. 9). Remarkably, we observed that *mga2Δ* cells displayed a defect in the nuclear accumulation of Aft1 upon iron depletion, which instead mislocalized to the vacuole (Fig. 9). The Aft1 localization defect of *mga2Δ* cells was due to low UFA levels since it was fully reverted by the addition of linoleic acid (Fig. 9). Curiously, the supplementation with linoleic acid did not alter Aft1 protein levels but improved the nuclear localization of Aft1 under iron-deficient conditions displayed by wild-type cells, suggesting that the UFA concentration of yeast cells under low iron is not the best for Aft1 function. In fact, wild-type cells slightly increase Aft1 accumulation into the vacuole upon iron depletion (Fig. 9). Interestingly, we have observed that the constitutively active *AFT1-1^{up}* allele restores both the iron regulon expression and the growth defect of *mga2Δ* cells under iron-deficient conditions (Fig. 10). Aft1-1^{up} protein contains a mutation in cysteine 291, which makes it insensitive to the iron signal generated in the mitochondria of iron replete cells, and consequently it is constitutively retained in the nucleus activating transcription [25, 26]. Therefore, somehow the Aft1-1^{up} protein bypasses the problem exhibited by *mga2Δ* cells under iron deprivation. But, more important, the rescue of *mga2Δ* growth defect on iron-deficient media by the *AFT1-1^{up}* allele indicates that the main consequence of the alteration in UFA/SFA is a defect in Aft1 localization.

Metals and lipid metabolism are interconnected at multiple levels. A previous study has shown that excess zinc activates the expression of the iron regulon via Aft1 and the low oxygen response via Mga2 [46]. Among Mga2 targets, the authors found *IZH4*, which belongs to the *IZH* family of genes encoding for membrane proteins implicated in zinc ion homeostasis and lipid metabolism [46]. Interestingly, this study also showed that a LORE reporter gene was activated in cells lacking *AFT1* [46], probably due to a decrease in intracellular iron levels that would promote the release of Mga2 from the ER membrane [19]. Iron and lipid metabolisms are also highly connected. For instance, the synthesis of ergosterol (the yeast cholesterol) depends on iron at four enzymatic steps within the late ergosterol pathway: Erg11 (lanosterol 14α-demethylase), its activator Dap1 and Erg5 (sterol C-22 desaturase) use heme as an essential cofactor, whereas Erg25 (C4-methyl sterol oxidase) and Erg3 (sterol C-5 desaturase) are oxo-diiron-dependent enzymes (reviewed in [47]). Thus, under iron-deficient conditions sterol intermediates, such as squalene and lanosterol, accumulate at the expense of ergosterol [20]. A crosstalk between ergosterol metabolism, iron regulation and ER stress has also been reported. Specifically, ER stresses have been shown to promote the translocation of Aft1 to the nucleus, whereas the addition of inhibitors of ergosterol biosynthesis, such as fluconazole or terbinafine, limits this Aft1 nuclear accumulation [48]. Opposite to our observations (Fig. 9), no accumulation of Aft1 in the vacuole has been reported in this case [48]. Sphingolipid biosynthesis also depends on iron at two enzymatic steps: Sur2 (sphinganine C4-hydroxylase), which catalyzes the conversion of sphinganine to phytosphingosine, and Scs7 (sphingolipid α-hydroxylase), which functions in the α-hydroxylation of

sphingolipid-associated very long chain fatty acids. Therefore, iron depletion alters the sphingolipid synthesis pathway [20]. Moreover, a recent report has shown that Mpo1 is a novel iron-dependent dioxygenase involved in phytosphingosine metabolism [49, 50]. Various studies suggest that sphingolipid metabolism could also modulate Aft1 function. For instance, yeast cells lacking the sphingomielinase ortholog Isc1, which hydrolyzes complex sphingolipids to produce ceramide, activate the iron regulon [34]. Moreover, a recent lipidomic and transcriptomic analysis of yeast cells has shown that overexpression of the alkaline dihydroceramidase *YDC1*, which promotes the hydrolysis of dihydroceramides, increases the expression of *AFT1* and, probably, of the iron regulon [51]. These results support the role played by lipids in the activation of Aft1 transcription factor.

Deletion of *MGA2* leads to a broad decrease in UFA levels that may affect the properties of many cellular membranes. In fact, the localization of ER and Golgi protein markers has shown that membrane transport is disrupted in *mga2Δ* cells due to a defect in UFA synthesis [52]. Electron microscopy has revealed a separation between the inner and outer nuclear membranes in *mga2Δ* cells that is accompanied by an aberrant nuclear membrane morphology characterized by the formation of sinusoidal proliferations on the outer nuclear membrane and vesicle-like projections in the intermembrane space, which are reversed by exogenous UFA addition [16, 39]. Although the consequences of these nuclear membrane defects are unknown, it is possible that the low UFA levels of *mga2Δ* cells under iron starvation conditions affect the properties of the nuclear and other membranes leading to Aft1 mislocalization. Further studies on the lipid composition of specific cellular

membranes will contribute to elucidate the molecular reasons for the misregulation of the Aft1 transcription factor.

In this report, we have uncovered that the growth defects of yeast *mga2Δ* cells under iron deficiency, which are reverted by ectopic *OLE1* expression or UFA supplementation [19], are due to a defective transport of the Aft1 transcription factor from the cytoplasm to the nucleus (see Fig. 11 for a model). Further studies would be necessary to elucidate how low UFA levels lead the accumulation Aft1 transcription factor into the vacuole.

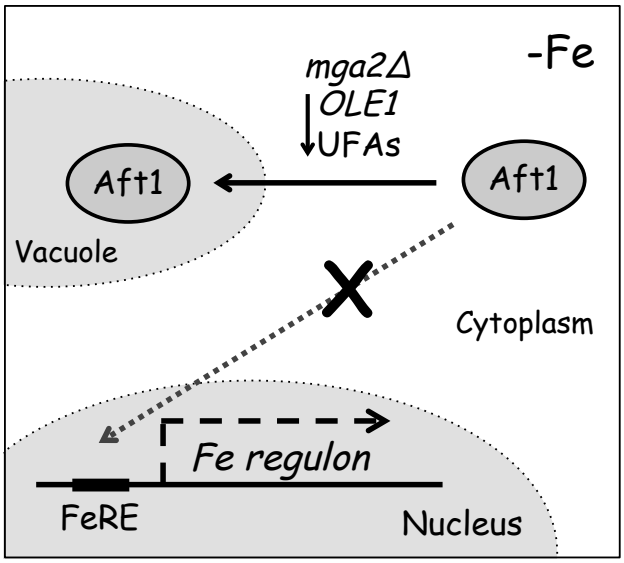

Fig. 11. A model for the defective activation of the iron regulon in *mga2Δ* cells. Yeast cells lacking the Mga2 transcription factor exhibit a defect in the expression of the Δ9-fatty acid desaturase *OLE1* gene when iron is scarce. As a consequence, the levels of UFAs dramatically decrease leading to a mislocalization of the iron-responsive transcription factor Aft1 to the vacuole instead of the nucleus. The defective activation of the iron regulon in *mga2Δ* cells causes a severe growth defect under iron-deficient conditions.

5. Acknowledgments

This work was supported by a predoctoral contract from the Regional Government of Valencia “Generalitat Valenciana” to Tania Jordá, and the Spanish Ministry of Science, Innovation and Universities (MICINN) grant BIO2017-87828-C2-1-P and FEDER (Fondo Europeo de Desarrollo Regional) funds to Sergi Puig. We are grateful to the members of the Iron Homeostasis laboratory, especially to María Teresa Martínez-Pastor, Lucia Ramos-Alonso, María González and Pilar Miró for technical and scientific assistance. We are also in debt with Drs. Dieter H. Wolf, Stefan Jentsch, Pamela Silver, Enrique Herrero, Dennis R. Winge, Jerry Kaplan, Kazuhiro Iwai and Martin Funk for providing yeast strains and plasmids used in this study.

Conflict of interest: The authors declare that no conflict of interest exists.

6. References

[1] R. Ernst, S. Ballweg, I. Levental, Cellular mechanisms of physicochemical membrane homeostasis, Curr Opin Cell Biol, 53 (2018) 44-51.
[2] P. Singh, Budding Yeast: An Ideal Backdrop for In vivo Lipid Biochemistry, Front Cell Dev Biol, 4 (2017) 156.
[3] J.E. Stukey, V.M. McDonough, C.E. Martin, Isolation and characterization of OLE1, a gene affecting fatty acid desaturation from Saccharomyces cerevisiae, J Biol Chem, 264 (1989) 16537-16544.
[4] P.S. Aguilar, D. de Mendoza, Control of fatty acid desaturation: a mechanism conserved from bacteria to humans, Mol Microbiol, 62 (2006) 1507-1514.
[5] C.E. Martin, C.S. Oh, Y. Jiang, Regulation of long chain unsaturated fatty acid synthesis in yeast, Biochim Biophys Acta, 1771 (2007) 271-285.
[6] S. Ballweg, R. Ernst, Control of membrane fluidity: the OLE pathway in focus, Biol Chem, 398 (2017) 215-228.
[7] R. Chellappa, P. Kandasamy, C.S. Oh, Y. Jiang, M. Vemula, C.E. Martin, The membrane proteins, Spt23p and Mga2p, play distinct roles in the activation of Saccharomyces cerevisiae OLE1 gene expression. Fatty acid-mediated regulation of Mga2p activity is independent of its proteolytic processing into a soluble transcription activator, J Biol Chem, 276 (2001) 43548-43556.
[8] T. Hoppe, K. Matuschewski, M. Rape, S. Schlenker, H.D. Ulrich, S. Jentsch, Activation of a membrane-bound transcription factor by regulated ubiquitin/proteasome-dependent processing, Cell, 102 (2000) 577-586.
[9] A.L. Hitchcock, H. Krebber, S. Frietze, A. Lin, M. Latterich, P.A. Silver, The conserved npl4 protein complex mediates proteasome-dependent membrane-bound transcription factor activation, Mol Biol Cell, 12 (2001) 3226-3241.
[10] M. Rape, T. Hoppe, I. Gorr, M. Kalocay, H. Richly, S. Jentsch, Mobilization of processed, membrane-tethered SPT23 transcription factor by CDC48(UFD1/NPL4), a ubiquitin-selective chaperone, Cell, 107 (2001) 667-677.
[11] N. Shcherbik, D.S. Haines, Cdc48p(Npl4p/Ufd1p) binds and segregates membrane-anchored/tethered complexes via a polyubiquitin signal present on the anchors, Mol Cell, 25 (2007) 385-397.
[12] N. Shcherbik, T. Zoladek, J.T. Nickels, D.S. Haines, Rsp5p is required for ER bound Mga2p120 polyubiquitination and release of the processed/tethered transactivator Mga2p90, Curr Biol, 13 (2003) 1227-1233.
[13] Y. Jiang, M.J. Vasconcelles, S. Wretzel, A. Light, L. Gilooly, K. McDaid, C.S. Oh, C.E. Martin, M.A. Goldberg, Mga2p processing by hypoxia and unsaturated fatty acids in Saccharomyces cerevisiae: impact on LORE-dependent gene expression, Eukaryot Cell, 1 (2002) 481-490.
[14] Y. Nakagawa, N. Sakumoto, Y. Kaneko, S. Harashima, Mga2p is a putative sensor for low temperature and oxygen to induce OLE1 transcription in Saccharomyces cerevisiae, Biochem Biophys Res Commun, 291 (2002) 707-713.
[15] Y. Jiang, M.J. Vasconcelles, S. Wretzel, A. Light, C.E. Martin, M.A. Goldberg, MGA2 is involved in the low-oxygen response element-dependent hypoxic induction of genes in Saccharomyces cerevisiae, Mol Cell Biol, 21 (2001) 6161-6169.
[16] M.A. Surma, C. Klose, D. Peng, M. Shales, C. Mrejen, A. Stefanko, H. Braberg, D.E. Gordon, D. Vorkel, C.S. Ejsing, R. Farese, Jr., K. Simons, N.J. Krogan, R. Ernst, A lipid E-MAP identifies Ubx2 as a critical regulator of lipid saturation and lipid bilayer stress, Mol Cell, 51 (2013) 519-530.
[17] S. Ballweg, E. Sezgin, M. Doktorova, R. Covino, J. Reinhard, D. Wunnicke, I. Hanelt, I. Levental, G. Hummer, R. Ernst, Regulation of lipid saturation without sensing membrane fluidity, Nat Commun, 11 (2020) 756.

[18] R. Covino, S. Ballweg, C. Stordeur, J.B. Michaelis, K. Puth, F. Wernig, A. Bahrami, A.M. Ernst, G. Hummer, R. Ernst, A Eukaryotic Sensor for Membrane Lipid Saturation, Mol Cell, 63 (2016) 49-59.
[19] A.M. Romero, T. Jorda, N. Rozes, M.T. Martinez-Pastor, S. Puig, Regulation of yeast fatty acid desaturase in response to iron deficiency, Biochim Biophys Acta Mol Cell Biol Lipids, 1863 (2018) 657-668.
[20] M. Shakoury-Elizeh, O. Protchenko, A. Berger, J. Cox, K. Gable, T.M. Dunn, W.A. Prinz, M. Bard, C.C. Philpott, Metabolic response to iron deficiency in *Saccharomyces cerevisiae*, J Biol Chem, 285 (2010) 14823-14833.
[21] C.D. Kaplan, J. Kaplan, Iron acquisition and transcriptional regulation, Chem Rev, 109 (2009) 4536-4552.
[22] O.S. Chen, R.J. Crisp, M. Valachovic, M. Bard, D.R. Winge, J. Kaplan, Transcription of the yeast iron regulon does not respond directly to iron but rather to iron-sulfur cluster biosynthesis, J Biol Chem, 279 (2004) 29513-29518.
[23] J.C. Rutherford, L. Ojeda, J. Balk, U. Muhlenhoff, R. Lill, D.R. Winge, Activation of the iron regulon by the yeast Aft1/Aft2 transcription factors depends on mitochondrial but not cytosolic iron-sulfur protein biogenesis, J Biol Chem, 280 (2005) 10135-10140.
[24] Y. Yamaguchi-Iwai, R. Ueta, A. Fukunaka, R. Sasaki, Subcellular localization of Aft1 transcription factor responds to iron status in *Saccharomyces cerevisiae*, J Biol Chem, 277 (2002) 18914-18918.
[25] R. Ueta, N. Fujiwara, K. Iwai, Y. Yamaguchi-Iwai, Iron-induced dissociation of the Aft1p transcriptional regulator from target gene promoters is an initial event in iron-dependent gene suppression, Mol Cell Biol, 32 (2012) 4998-5008.
[26] Y. Yamaguchi-Iwai, A. Dancis, R.D. Klausner, AFT1: a mediator of iron regulated transcriptional control in *Saccharomyces cerevisiae*, EMBO J, 14 (1995) 1231-1239.
[27] Y. Yamaguchi-Iwai, R. Stearman, A. Dancis, R.D. Klausner, Iron-regulated DNA binding by the AFT1 protein controls the iron regulon in yeast, EMBO J, 15 (1996) 3377-3384.
[28] C.C. Philpott, O. Protchenko, Response to iron deprivation in Saccharomyces cerevisiae, Eukaryot Cell, 7 (2008) 20-27.
[29] N. Sanvisens, S. Puig, Causes and consequences of nutritional iron deficiency in living organisms, in: T.C. Merkin (Ed.) Biology of starvation in humans and other organisms, Nova Science Publishers, Place Published, 2011, pp. 245-276.
[30] N. Sanvisens, A.M. Romero, X. An, C. Zhang, R. de Llanos, M.T. Martinez-Pastor, M.C. Bano, M. Huang, S. Puig, Yeast Dun1 kinase regulates ribonucleotide reductase inhibitor Sml1 in response to iron deficiency, Mol Cell Biol, 34 (2014) 3259-3271.
[31] V.V. Kushnirov, Rapid and reliable protein extraction from yeast, Yeast, 16 (2000) 857-860.
[32] M. Gomar-Alba, P. Alepuz, M. del Olmo, Dissection of the elements of osmotic stress response transcription factor Hot1 involved in the interaction with MAPK Hog1 and in the activation of transcription, Biochim Biophys Acta, 1829 (2013) 1111-1125.
[33] S. Puig, M. Lau, D.J. Thiele, Cti6 is an Rpd3-Sin3 histone deacetylase-associated protein required for growth under iron-limiting conditions in Saccharomyces cerevisiae, J Biol Chem, 279 (2004) 30298-30306.
[34] T. Almeida, M. Marques, D. Mojzita, M.A. Amorim, R.D. Silva, B. Almeida, P. Rodrigues, P. Ludovico, S. Hohmann, P. Moradas-Ferreira, M. Corte-Real, V. Costa, Isc1p plays a key role in hydrogen peroxide resistance and chronological lifespan through modulation of iron levels and apoptosis, Mol Biol Cell, 19 (2008) 865-876.
[35] T.S. Martins, V. Costa, C. Pereira, Signaling pathways governing iron homeostasis in budding yeast, Mol Microbiol, (2018).
[36] B. Samanfar, K. Omidi, M. Hooshyar, B. Laliberte, M. Alamgir, A.J. Seal, E. Ahmed-Muhsin, D.F. Viteri, K. Said, F. Chalabian, A. Golshani, G. Wainer, D. Burnside, K. Shostak, M. Bugno, W.G. Willmore, M.L. Smith, A. Golshani, Large-scale investigation of oxygen response mutants in Saccharomyces cerevisiae, Mol Biosyst, 9 (2013) 1351-1359.

[37] M. Costanzo, A. Baryshnikova, J. Bellay, Y. Kim, E.D. Spear, C.S. Sevier, H. Ding, J.L. Koh, K. Toufighi, S. Mostafavi, J. Prinz, R.P. St Onge, B. VanderSluis, T. Makhnevych, F.J. Vizeacoumar, S. Alizadeh, S. Bahr, R.L. Brost, Y. Chen, M. Cokol, R. Deshpande, Z. Li, Z.Y. Lin, W. Liang, M. Marback, J. Paw, B.J. San Luis, E. Shuteriqi, A.H. Tong, N. van Dyk, I.M. Wallace, J.A. Whitney, M.T. Weirauch, G. Zhong, H. Zhu, W.A. Houry, M. Brudno, S. Ragibizadeh, B. Papp, C. Pal, F.P. Roth, G. Giaever, C. Nislow, O.G. Troyanskaya, H. Bussey, G.D. Bader, A.C. Gingras, Q.D. Morris, P.M. Kim, C.A. Kaiser, C.L. Myers, B.J. Andrews, C. Boone, The genetic landscape of a cell, Science, 327 (2010) 425-431.
[38] J. Zheng, J.J. Benschop, M. Shales, P. Kemmeren, J. Greenblatt, G. Cagney, F. Holstege, H. Li, N.J. Krogan, Epistatic relationships reveal the functional organization of yeast transcription factors, Mol Syst Biol, 6 (2010) 420.
[39] S. Zhang, Y. Skalsky, D.J. Garfinkel, MGA2 or SPT23 is required for transcription of the delta9 fatty acid desaturase gene, OLE1, and nuclear membrane integrity in Saccharomyces cerevisiae, Genetics, 151 (1999) 473-483.
[40] M. Courel, S. Lallet, J.M. Camadro, P.L. Blaiseau, Direct activation of genes involved in intracellular iron use by the yeast iron-responsive transcription factor Aft2 without its paralog Aft1, Mol Cell Biol, 25 (2005) 6760-6771.
[41] S. Puig, E. Askeland, D.J. Thiele, Coordinated remodeling of cellular metabolism during iron deficiency through targeted mRNA degradation, Cell, 120 (2005) 99-110.
[42] R.J. Crisp, A. Pollington, C. Galea, S. Jaron, Y. Yamaguchi-Iwai, J. Kaplan, Inhibition of heme biosynthesis prevents transcription of iron uptake genes in yeast, J Biol Chem, 278 (2003) 45499-45506.
[43] J.C. Rutherford, S. Jaron, D.R. Winge, Aft1p and Aft2p mediate iron-responsive gene expression in yeast through related promoter elements, J Biol Chem, 278 (2003) 27636-27643.
[44] P.L. Blaiseau, E. Lesuisse, J.M. Camadro, Aft2p, a novel iron-regulated transcription activator that modulates, with Aft1p, intracellular iron use and resistance to oxidative stress in yeast, J Biol Chem, 276 (2001) 34221-34226.
[45] J.C. Rutherford, S. Jaron, E. Ray, P.O. Brown, D.R. Winge, A second iron-regulatory system in yeast independent of Aft1p, Proc Natl Acad Sci USA, 98 (2001) 14322-14327.
[46] T.J. Lyons, N.Y. Villa, L.M. Regalla, B.R. Kupchak, A. Vagstad, D.J. Eide, Metalloregulation of yeast membrane steroid receptor homologs, Proc Natl Acad Sci U S A, 101 (2004) 5506-5511.
[47] Z. Hu, B. He, L. Ma, Y. Sun, Y. Niu, B. Zeng, Recent Advances in Ergosterol Biosynthesis and Regulation Mechanisms in Saccharomyces cerevisiae, Indian J Microbiol, 57 (2017) 270-277.
[48] N. Cohen, M. Breker, A. Bakunts, K. Pesek, A. Chas, J. Argemi, A. Orsi, L. Gal, S. Chuartzman, Y. Wigelman, F. Jonas, P. Walter, R. Ernst, T. Aragon, E. van Anken, M. Schuldiner, Iron affects Ire1 clustering propensity and the amplitude of endoplasmic reticulum stress signaling, J Cell Sci, 130 (2017) 3222-3233.
[49] N. Seki, K. Mori, T. Kitamura, M. Miyamoto, A. Kihara, Yeast Mpo1 Is a Novel Dioxygenase That Catalyzes the alpha-Oxidation of a 2-Hydroxy Fatty Acid in an Fe(2+)-Dependent Manner, Mol Cell Biol, 39 (2019).
[50] T. Kitamura, N. Seki, A. Kihara, Phytosphingosine degradation pathway includes fatty acid alpha-oxidation reactions in the endoplasmic reticulum, Proc Natl Acad Sci U S A, 114 (2017) E2616-E2623.
[51] D.J. Montefusco, L. Chen, N. Matmati, S. Lu, B. Newcomb, G.F. Cooper, Y.A. Hannun, X. Lu, Distinct signaling roles of ceramide species in yeast revealed through systematic perturbation and systems biology analyses, Sci Signal, 6 (2013) rs14.
[52] R. Burr, E.V. Stewart, P.J. Espenshade, Coordinate Regulation of Yeast Sterol Regulatory Element-binding Protein (SREBP) and Mga2 Transcription Factors, J Biol Chem, 292 (2017) 5311-5324.

Supplemental Tables

Supplemental Table S1. List of yeast strains and plasmids used in this study.

Strain or plasmid	Description	Source
Strains		
BY4741	*MATa his3Δ1 leu2Δ0 met15Δ0 ura3Δ0*	Invitrogen
SPY824	BY4741 *mga2::KanMX4*	Invitrogen
SPY823	BY4741 *spt23::KanMX4*	Invitrogen
SPY28	BY4741 *aft1::KanMX4*	Invitrogen
SPY992	BY4741 *aft1::KanMX4 mga2:HisMX6*	This study
YWO0607	*MATa ura3 leu2-3,112 his3-11,15 Gal*$^{+}$	D. H. Wolf
YWO0608	YWO0607 *pre1-1*	D. H. Wolf
YWO1	*MATa his3-Δ200, leu2-3,112, lys2-801, trp1-1(am), ura3-52*	[8]
Y0356	YWO1 *rsp5::HIS3; ura3-52::RSP5::URA3*	[8]
Y0358	YWO1 *rsp5::HIS3; ura3-52::rps5-2::URA3*	[8]
PSY580	*MATa ura3-52 leu2Δ1 trp1Δ63*	[9]
PSY2340	PSY580 *npl4-1*	[9]
Plasmids		
pRS416	CEN *URA3*	M. Funk
pRS316-P_{GAL1}-OLE1	CEN *URA3* P_{GAL1}*-OLE1*	[8]

pPS2364	CEN *URA3 MGA2*	[9]
pPS2358	CEN *URA3 MGA2ΔTM*	[9]
P_{FET3}-lacZ	CEN *URA3* P_{FET3}*-lacZ*	J. Kaplan
pSP441	CEN *URA3* $P_{CYC1\text{-}FeRE}$*-lacZ*	[41]
JK1346	2 μm *URA3 GFP-AFT1*	J. Kaplan
pRS416-AFT1-12HA	CEN *URA3 AFT1-12HA*	[25]
pRS416-AFT1-1^{up}-12HA	CEN *URA3 AFT1-*1^{up}*(C291F)-12HA*	[25]

Supplemental Table S2. Oligonucleotides used for RT-qPCR in this work.

Name	***Sequence (from 5' to 3')***
FET3-qPCR-F	TGACCGTTTTGTCTTCAGGT
FET3-qPCR-R	CTCCACGATTTCATCCTTCTC
FTR1-qPCR-F	GGTCACTTGCCTTTCACCAA
FTR1-qPCR-R	TTGCTCTTCCGTCAACTCCT
FIT3-qPCR-F	CATCCTCTAGCACCGCTGAA
FIT3-qPCR-R	CAATAACATGACGGCAGCAA
ARN2-qPCR-F	TTCCTTTCGCTCCATTCAAG
ARN2-qPCR-R	GAGATACCCAGCAGCCATTT
FIT1-qPCR-F	TCTAGGGATGCCCAATCTGT
FIT1-qPCR-R	ACCAGCGGTAGTGGTTTGA
OLE1-qPCR-F	TCGACAAGAAGGGAAACGAA
OLE1-qPCR-R	CATGGTTGTTCGGAGATGTG
PGK1-qPCR-F	AAGCGTGTCTTCATCAGAGTTG
PGK1-qPCR-R	CGTATCTTGGGTGGTGTTCC
FUS1-ChIP-prom-F	CATGTGGACCCTTTCAAAAC
FUS1-ChIP-prom-R	AGACAGCGCGAAAAGTGACA
FET3-ChIP-prom-F	TACTTTCCGGGTGCGAAT

FET3-ChIP-prom-R	TGGCGAGAATAAGAGCAC

Supplemental Figs.

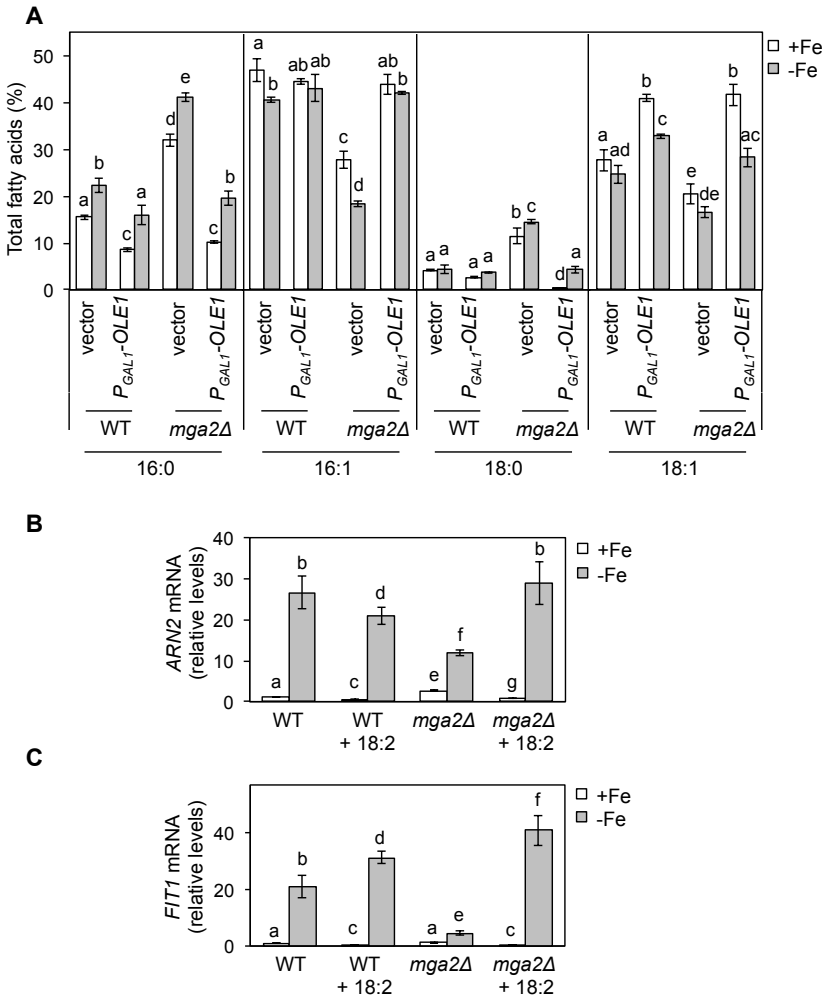

Supplemental Fig. S1. UFA supplementation reverts the iron regulon activation defect of *mga2Δ* cells. (A) The *GAL1*-driven expression of *OLE1* reverts the UFA synthesis defect of *mga2Δ* cells. Wild-type (WT, BY4741) cells transformed with pRS416 or pRS316-P_{GAL1}-OLE1 plasmids were cultivated as described in Fig. 6. The percentage of palmitic acid (16:0), estearic acid (18:0), palmitoleic acid (16:1) and oleic acid (18:1), was represented. (B-C) Wild-type (WT, BY4741) and *mga2Δ (*SPY824) cells were cultivated as in Fig. 6. Total RNA was extracted and *ARN2* (B) and *FIT2* (C) mRNA levels normalized with *PGK1* mRNA were determined by RT-qPCR. Transcript values are shown as relative to the WT (+Fe) samples. In all cases, data indicate the average and

standard deviation of three biologically independent experiments. Different letters above the bars represent significant differences (p-value < 0.05).

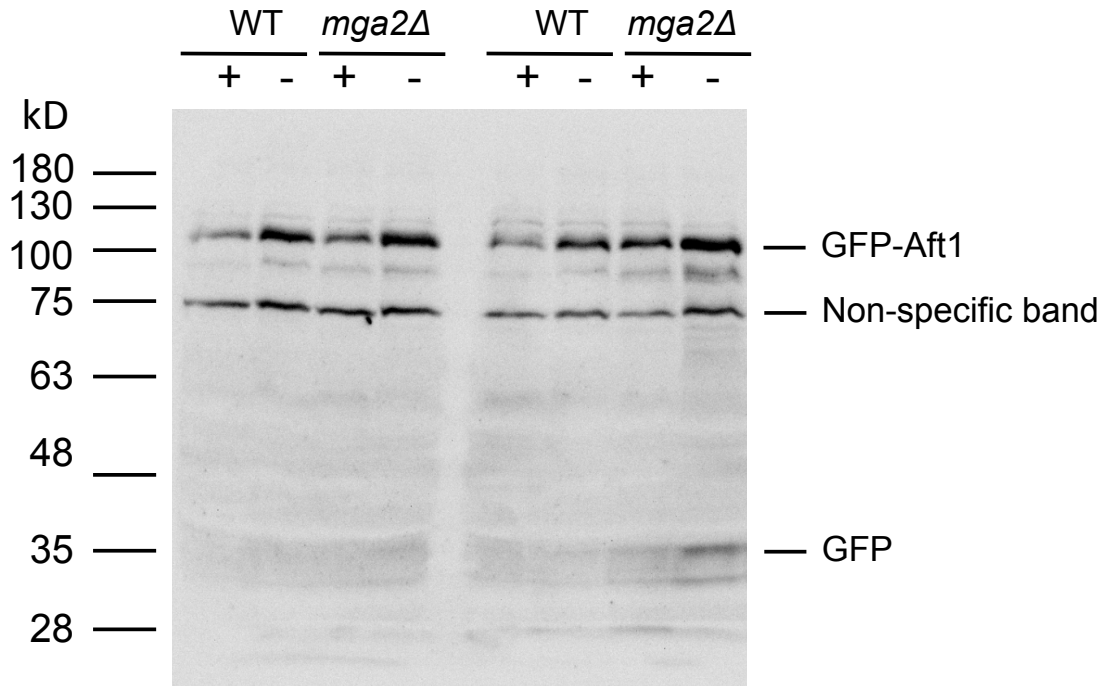

Supplemental Fig. S2. GFP-Aft1 protein levels. Wild-type (WT, BY4741) and *mga2Δ* (SPY824) cells containing JK1346 (pRS426-GFP-AFT1) plasmid were cultivated as in Fig. 9. GFP-Aft1 protein levels were analyzed by Western blot with anti-GFP antibody. A non-specific band and Ponceau S staining were used as loading controls. Two independent biological replicates are shown.

,